Available online at www.eccomasproceedia.org
Eccomas Proceedia UNCECOMP (2023) 500-510

ECCOMAS
Proceedia

UNCECOMP 2023
5th ECCOMAS Thematic Conference on
Uncertainty Quantification in Computational Science and Engineering
M. Papadrakakis, V. Papadopoulos, G. Stefanou (eds.)
Athens, Greece, 12-14 June 2023

APPLICATION OF MULTI-FIDELITY AND RANDOMIZED QUASI-MONTE CARLO METHODS IN THE PROBABILISTIC ASSESSMENT OF EXCAVATION-INDUCED BUILDING DAMAGES

Jinyan. Zhao[1] **and Matthew J. DeJong**[1]

[1] The Department of Civil and Environmental Engineering
University of California, Berkeley
e-mail: {jinyan_zhao,dejong}@berkeley.edu

Abstract

This paper presents an uncertainty quantification problem involving high-dimensional uncertainty inputs and a nonlinear structural analysis model. The uncertainty quantification problem can be considered a high-dimensional numerical integration with a nonlinear integrand. The crude Monte Carlo, multi-fidelity Monte Carlo, and randomized quasi-Monte Carlo methods are applied to solve the numerical integration problem, and numerical experiments are conducted to compare the efficiency of the Monte Carlo methods. It is shown that both multi-fidelity Monte Carlo and randomized quasi-Monte Carlo may significantly improve the efficiency of the studied problem. The randomized quasi-Monte Carlo method is easier to implement, but a carefully selected quasi-random sample and more sophisticated variance estimation are needed to successfully apply the randomized quasi-Monte Carlo method.

Keywords: Uncertainty quantification; Numerical integration; Monte Carlo; Multi-fidelity Monte Carlo; Randomized Quasi-Monte Carlo

1 INTRODUCTION

Due to complex and lengthy geological processes, e.g., deposition, sedimentation, metamorphism, weathering, and biological effects, the physical and mechanical properties of soil can have significant spatial variability. In tunnel and deep excavation engineering, random field (RF) models are more and more commonly used to analyze the effect of spatial variability on tunnel stability, braced support stability, and ground movements (e.g., [1-3]). Simulating an RF model in numerical analyses may require tens to hundreds of independent random variables (i.e., tens to hundreds of uncertainty input dimensions), and the forward propagation process of such high-dimension uncertainty can be a challenge. Monte Carlo (MC) methods generally

ISSN:2623-3339
Peer-review under responsibility of the organizing committee of UNCECOMP 2023.
doi: 10.7712/120223.10353.19824

show a dimension-independent convergence rate and are powerful for the uncertainty propagation of computational models involving high-dimensional uncertainty. As reviewed in [4], the crude MC method is the most adopted method for uncertainty propagation in tunneling and excavation engineering. However, the excessive calculation expanse in the crude MC method may prohibit practical engineers from utilizing uncertainty quantification in the analyses of soil spatial variability. In contrast, some advanced MC methods (such as variance reduction methods and quasi-MC methods) may significantly reduce the calculation expanse and can be used for high-dimensional uncertainty quantification in tunneling and excavation engineering and broader civil infrastructure engineering practice.

In this paper, the crude Monte Carlo (CMC), a multi-fidelity MC (MFMC) method, and a randomized quasi-MC method (RQMC) are applied in the uncertainty propagation of a deep excavation analysis, and their efficiencies are compared. Both MFMC and RQMC are relatively easy to implement and showed significant efficiency improvement, which demonstrates a promising application of the advanced MC methods. In section 2, a probabilistic excavation-structure interaction model involving RF models is presented and used as a benchmark problem for comparing the efficiency of the MC methods. In section 3, the MFMC and RQMC methods are briefly reviewed and applied to the benchmark problem. In section 4, the performance of the MFMC and RQMC methods is discussed. This paper demonstrates the benefit of using advanced MC methods in high-dimensional and nonlinear uncertainty quantification problems.

2 A HIGH DIMENSIONAL FORWARD PROPAGATION PROBLEM IN DEEP EXCAVATION ENGINEERING

The complete uncertainty propagation procedures are usually not reported in civil engineering uncertainty quantification research involving soil spatial variabilities. As a result, an uncertainty quantification study involving soil RF models and a nonlinear structural analysis model (SAM) is reviewed and used as a benchmark to analyze the performance of the advanced MC methods.

The probabilities of building damage induced by an adjacent deep excavation are estimated on a small community-level scale by Zhao et al. [5], as shown in Fig. 1. The SAM adopted in [5] is a customized hybrid finite element code called ASRE 3D [6] which takes the ground displacements, building geometries, soil stiffnesses, building stiffnesses, and building weights as inputs. The uncertainty inputs are an RF model of the excavation-induced ground displacement, an RF model of soil stiffnesses, and four random variables describing building stiffnesses and building weights. The ground displacement profile perpendicular to the wall is described with the profiles proposed in [7], which is determined by three parameters $d_{v,max}/H, \eta$, and $d_{l,max}/H$, as shown in Eq. (1). The spatial variabilities of $d_{v,max}/H$ and η along the excavation wall are investigated in [5] and described with two 1D lognormal RFs with Gaussian semivariogram functions. $d_{l,max}/H$ is modeled as $d_{v,max}/H$ multiplying a random variable as suggested in [8]. The soil stiffness (E_s) in the area is described by another lognormal RF model, with a scale of fluctuation (SOF) equal to 10 m, which corresponds to the worst-case SOF scenario of building differential settlement as suggested in [9]. The RF models adopted in this paper are stationary, and the mean values, coefficient of variances (CoVs), correlation functions, and SOFs are summarized in Table 1.

$$d_v = d_{v,max} \frac{1.14}{\frac{d}{H}+0.39} \frac{1}{0.46\sqrt{2\pi}} \exp\left(-\frac{\left(\ln\left(\frac{d}{H}+0.39\right)-0.095\right)^2}{0.423} \right) \tag{1a}$$

$$d_v = d_{l,max} \frac{2.14}{\frac{d}{H}+0.82} \frac{1}{0.44\sqrt{2\pi}} \exp\left(-\frac{\left(\ln\left(\frac{d}{H}+0.82\right)-0.80\right)^2}{0.387}\right) \quad (1b)$$

To generate RF samples, the RF models are first discretized at the N nodes at the soil-structure interface, as shown in Fig. 1(c). The realizations of $d_{v,max}/H, \eta$, and E_s are generated with the discrete Karhunen Loeve Expansion (KLE) method [10], where the covariance matrices (in the logarithmic space) of the discretized RFs are first calculated. The matrices are eigen decomposed, and the M largest eigenvalues accounting for 99% of the sum of all eigenvalues are selected. M independent random variables are then generated with the PCG64 pseudorandom number generator implemented in the Python package NumPy. The vector of M independent random variables is multiplied by the first M eigenvalues and then multiplied by the first M eigenvectors to form a realization of the RFs at the N nodes. An RF with a larger SOF and smaller CoV is more uniform and requires a smaller M to capture the variance in the model, while an RF with a smaller SOF and larger CoV shows a larger fluctuation, and a larger M is needed. In this study, the M values required for the simulation of $d_{v,max}/H, \eta$, and E_s are 4, 10, and 510. With another 6 independent variables describing the uncertainty in the estimated $d_{l,max}/d_{v,max}$, building stiffnesses, and building dead loads, the total uncertainty dimension of the studied model is 550. Given a realization of the RFs, the ground movements and soil stiffness matrix coefficients are calculated based on Eq. (1) and Mindlin's solutions at the discretized nodes and assigned to the SAM model. The outputs of the SAM are the characteristic strain (99% quantile of the strain in all elements) of the two buildings (ε_A and ε_B). The quantities of interest (QoIs) are the probabilities ($p_{f,A}$ and $p_{f,B}$) that ε_A and ε_B exceed the limit state strains (ε_{lim}), which are defined in [11].

RF	Distribution	Mean	CoV	Correlation function	SOF
$d_{v,max}/H$	Lognormal	0.1%	0.38	Gaussian	18 m
η	Lognormal	1.3	0.097	Gaussian	5 m
E_s	Lognormal	10 MPa	0.4	Exponential	10 m

Table 1: Random field models in the benchmark.

The crude MC method with 5000 simulations is conducted to estimate the QoIs. The adopted pseudorandom number generator PCG64 has a period of 2^{128}, which is greater than N_r^2, where N_r is the number of random numbers used in this study. As suggested in [12], a pseudorandom number generator with a period greater than N_r^2 is required to ensure the randomness behavior of the samples. The MT19937 (default in Matlab) pseudorandom number generator with a long period of $2^{19937}-1$ can be adopted if a larger N_r is needed in a study. The convergence and corresponding confidence intervals estimated from the asymptotic normal distribution can be found in Fig. 3 and 4. To enable fast simulation, ASRE 3D is computationally optimized by C++ optimizing compiler, sparse storage scheme, and high-performance linear solver. The time required for one model evaluation is around 108 seconds using a single CPU thread. As a comparison, an implementation of ASRE 3D in Matlab costs around 324 seconds for one model evaluation using multiple CPU threads. The optimized ASRE 3D can be installed in high-performance computer clusters, and 5000 MCS takes 2 hours, 6 minutes, and 35 seconds.

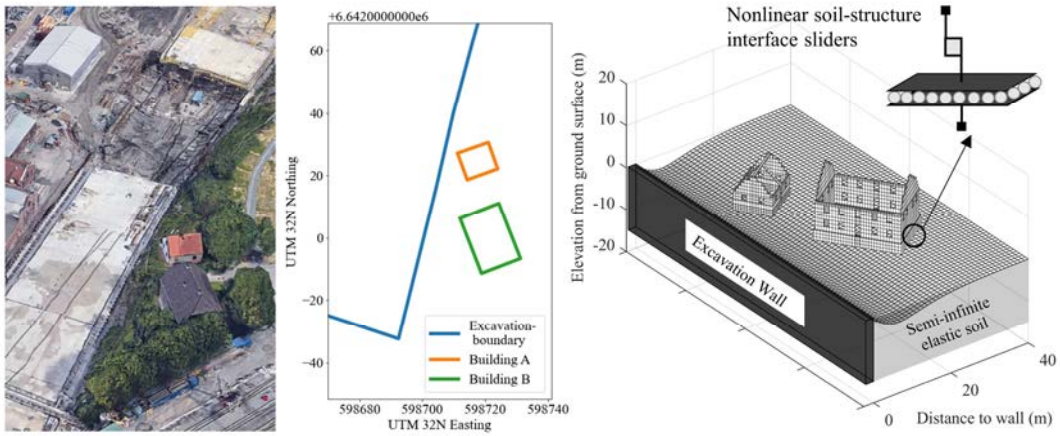

(a) (b) (c)

Figure 1: (a) Bird's eye view of the benchmark problem (from Google Earth); (b) Location of the excavation wall and studied buildings; (c) 3D soil-structure interaction structural analysis model.

3 APPLICATION OF ADVANCED MC METHODS: MULTI-FIDELITY MC AND RANDOMIZED QUASI-MC

3.1 Convergence and efficiency

The convergence of the crude MC method and the concept of efficiency are reviewed to analyze the performance of the MC methods. Let $\varepsilon = g(\boldsymbol{X})$ stands for the SAM, where $\boldsymbol{X}$ is a vector of the latent random variables used to generate the realizations of the RF and random variable inputs of the SAM. The QoI can be written as $p_f = P(\varepsilon > \varepsilon_{lim}) = E[I(\varepsilon > \varepsilon_{lim})] = E[f(\boldsymbol{X})]$. A crude MC estimator of p_f is defined as $Q_n = \frac{1}{n}\sum_{i=1}^{n} f(\boldsymbol{X}_i)$, which is also a random variable. The expectation of Q_n is $E[Q_n] = \frac{1}{n}\sum_{i=1}^{n} E[f(\boldsymbol{X}_i)] = E[f(\boldsymbol{X})] = p_f$. According to the central limit theorem, $\frac{Q_n - E[Q_n]}{\sigma/\sqrt{n}}$ convergence to the standard normal distribution (i.e., $\frac{Q_n - E[Q_n]}{\sigma/\sqrt{n}} \Rightarrow N(0,1)$), where $\sigma = \left(\int_{\Omega_X} (f(\boldsymbol{X}) - E[f(\boldsymbol{X})]) d\boldsymbol{X}\right)^{1/2}$. As a result, a confidence interval of Q_n in the form of Eq. (2) can be estimated based on the standard normal distribution of $\frac{Q_n - E[Q_n]}{\sigma/\sqrt{n}}$ when n is sufficiently large,

$$\left(Q_n \pm \frac{\sigma}{\sqrt{n}} z_{\alpha/2}\right) \tag{2}$$

Where $z_{\alpha/2}$ is the $1000(1-\alpha/2)$th percentile of the standard normal distribution, and σ can be estimated with the sample standard deviation $\hat{\sigma} = \left(\sum_{i=1}^{n} \frac{(f(\boldsymbol{X}_i) - Q_n)^2}{n-1}\right)^{1/2}$. It can be observed that the confidence interval shrinks in a rate of $\frac{\sigma}{\sqrt{n}}$, and the convergence rate of Q_n is usually considered in the order of $O(1/\sqrt{n})$ [13]. It can also be observed that the convergence rate is independent of the dimension of $\boldsymbol{X}$, which makes Q_n preferred for high-dimension uncertainty quantification over surrogate modeling methods.

A convergence proportional to $\frac{\sigma}{\sqrt{n}}$ is often considered too slow, and advanced MC methods seek to improve the convergence rate in two paths. The first is to reduce the magnitude of σ, which is often referred to as variance reduction techniques, and the second path is referred to as quasi-MC, which uses a deterministic sequence of numbers (often called quasi-random or

low-discrepancy samples) to replace the pseudorandom numbers in the crude MC. The low-discrepancy samples are designed to be more uniform than pseudorandom samples, especially when the sample size is small, and the convergence rate of the quasi-MC estimators for sufficiently smooth integrands can be as high as $O(n^{-3/2}\log_{s/2} n)$, where s is the dimension of $\boldsymbol{X}$ [13]. Low-discrepancy samples, such as lattice sequences, Halton sequences, and Sobol's sequences, are hard to design when the dimension of $\boldsymbol{X}$ is large, however, recent research [14-15] constructed Sobol's sequences with dimensions up to 21201. In this paper, the performance of a variance reduction technique using the Multi-fidelity MC (MFMC) method and a randomized quasi-MC (RQMC) method using Sobol's quasi-random sampling are studied.

The concept of efficiency [16] is adopted to describe the performance of the MC methods. The efficiency of an estimator $\hat{\mu}$ for a quantify μ is given by:

$$\mathrm{Eff}(\hat{\mu}) = [\mathrm{MSE}(\hat{\mu}) \times \mathrm{C}(\hat{\mu})]^{-1} \tag{3}$$

Where $\mathrm{MSE}(\hat{\mu}) = \mathrm{Var}(\hat{\mu}) + \mathrm{Bias}^2(\hat{\mu})$ is the mean-square error of $\hat{\mu}$ and $\mathrm{C}(\hat{\mu})$ is the expected computation time for $\hat{\mu}$. For a crude MC estimator Q_n, $\mathrm{Bias}^2(Q_n)$ is zero, $\mathrm{Var}(Q_n) = \sigma^2/n$ (see Eq. (2)), and $\mathrm{C}(Q_n) = cn$, where c is the cost for single SAM evaluation and n is the number of samples. As a result, $\mathrm{Eff}(Q_n) = \left[\frac{\sigma^2}{n} \times cn\right]^{-1} = [\sigma^2 c]^{-1}$, which is independent with the sample size, i.e., increasing sample size does not increase efficiency for the crude MC method. To achieve better efficiency, a faster reduction of $\mathrm{MSE}(\hat{\mu})$ than the increase of $\mathrm{C}(\hat{\mu})$ is needed. Because efficiency considers both MSE and computation expense, it is used to compare the performance of the MC methods in this paper.

3.2 A MFMC method

The MFMC method studied in this paper is based on the control variate framework. Given a crude MC estimator $Q_n = \frac{1}{n}\sum_{i=1}^{n} f(\boldsymbol{X}_i)$, the control variate method calibrates Q_n by the error of another MC estimator $Q_{c,n} = \frac{1}{n}\sum_{i=1}^{n} h(\boldsymbol{X}_i)$, where $h(\boldsymbol{X})$ is positively correlated to $f(\boldsymbol{X})$ and $E[h(\boldsymbol{X})]$ is known or cheaper to compute. Because $h(\boldsymbol{X})$ and $f(\boldsymbol{X})$ are positively correlated, Q_n is likely to be overestimating $E[f(\boldsymbol{X})]$ if $Q_{c,n}$ is larger than $E[h(\boldsymbol{X})]$. Since $E[h(\boldsymbol{X})]$ is known or cheap, the error of $Q_{c,n}$ can be estimated cheaply and Q_n can be calibrated to reduce the variance/MSE of Q_n with a low computation cost. More specifically, a control variate estimator $Q_{cv,n}$ is defined as:

$$Q_{cv,n} = \frac{1}{n}\sum_{i=1}^{n}\{f(\boldsymbol{X}_i) + \beta\big(E[h(\boldsymbol{X}_i)] - h(\boldsymbol{X}_i)\big)\} \tag{4}$$

Where β is a constant to be determined. It can be proved that $Q_{cv,n}$ is unbiased because $E\big[f(\boldsymbol{X}_i) + \beta\big(E[h(\boldsymbol{X}_i)] - h(\boldsymbol{X}_i)\big)\big] = E[f(\boldsymbol{X}_i)] + \beta E[E[h(\boldsymbol{X}_i)] - h(\boldsymbol{X}_i)] = E[f(\boldsymbol{X}_i)] + \beta(E[h(\boldsymbol{X}_i)] - E[h(\boldsymbol{X}_i)]) = E[f(\boldsymbol{X})]$. In addition, it can also be proved that $\mathrm{Var}(Q_{cv,n})$ is minimized when $\beta = \beta^* = \frac{\mathrm{COV}(f(\boldsymbol{X}),h(\boldsymbol{X}))}{\mathrm{Var}(h(\boldsymbol{X}))}$, and $\mathrm{Var}\big(Q_{cv,n}\big) = \frac{1}{n(n-1)}\sum_{i=1}^{n}\big(f(\boldsymbol{X}_i) + \beta^*\big(E[h(\boldsymbol{X}_i)] - h(\boldsymbol{X}_i)\big) - Q_{cv,n}\big)^2$ [16]. In practice, the covariance $\mathrm{COV}\big(f(\boldsymbol{X}), h(\boldsymbol{X})\big)$ is usually unknown. Therefore, a small number r of pilot simulations can be used to estimate the β^* with:

$$\hat{\beta} = \frac{\sum_{i=1}^{r} f(\boldsymbol{X}_i)\cdot h(\boldsymbol{X}_i) - r(Q_r \cdot QC_r)}{(r-1)\mathrm{Var}\big(h(\boldsymbol{X}_i)\big)} \tag{5}$$

In the benchmark problem, $f(\boldsymbol{X})$ is the nonlinear SAM ASRE 3D. If a rigid connection is assumed at the soil-structure interface and the nonlinear sliders (see Fig.(1c)) are deactivated, a linear model can be obtained. The linear model can be considered a lower-fidelity model of

ASRE 3D and is much cheaper to evaluate. The linear (lower fidelity) and nonlinear (higher fidelity) models are strongly correlated, and the linear model is used as $h(\boldsymbol{X})$ in this paper. Because multiple fidelity models are used in the MC method, this method is called the multi-fidelity MC method in many engineering communities (e.g., [17-19]). $h(\boldsymbol{X})$ can be estimated with a much smaller computation expanse (40 seconds), and 5000 crude MC simulation is done first to estimate $E[h(\boldsymbol{X})]$. Afterward, 200 pilot simulation ($r = 200$) is adopted to estimate $\hat{\beta}$, and another 4800 MC simulations are conducted to calculate an MFMC estimator with Eq. (4). The convergence and efficiency of the MFMC estimator are discussed in section 3.4.

3.3 A randomized quasi-MC method.

Quasi-MC methods use low-discrepancy point sets that behave more similarly to multi-variate uniform distribution than pseudorandom samples when the dimension is high and the sample size is relatively small. In fact, discrepancy (e.g., the star discrepancy defined in [20]) is a group of measures that describe the distinction between the empirical distribution of a point set and multi-variate uniform distribution. It is widely recognized that in numerical integration, the trapezoidal and quadrature rules provide faster convergence than random samples when the integral dimension is low. This is because the design of experiment (DOE) points in trapezoidal/quadrature rules are more uniformly distributed (i.e., have lower discrepancy) than random sample points. However, as the integral dimension increases, trapezoidal/quadrature rules construct DOE points with a complete combination or product rule, and the number of DOE points increases exponentially with dimension. As a result, the number of integrand evaluations in trapezoidal/quadrature rules is not affordable in high-dimensional integral, and this phenomenon is called the "curse of dimensionality" [21]. Fig. (2a) is a plot of 64 DOE points for the trapezoidal rule in two dimensions, and it can be observed that the points in the same column/row have the same first/second coordinate. In contrast, points in crude MC samples or low-discrepancy point sets have distinct coordinates when they are projected on each dimension, as illustrated in Fig. (2b-2d), so that the integrand $f(\boldsymbol{X})$ is evaluated at more locations with a small sample size under high dimensionality. Moreover, low-discrepancy point sets (e.g., Fig. (2c) and Fig. (2d)) are designed such that the projection of the points on each coordinate distributes more evenly than crude MC sample points. As a result, low-discrepancy sample points take advantage of both trapezoidal/quadrature rules and crude MC method to achieve fast numerical integration. An estimator $Q_{qmc} = \frac{1}{n}\sum_{i=1}^{n} f(\widetilde{\boldsymbol{X}_i})$, where $\widetilde{\boldsymbol{X}_i}$ are points in a low-discrepancy point set (P_n), is called a Quasi-MC estimator. The lattices method and digit sequence/digit net are two groups of methods to construct low-discrepancy samples, and a digit sequence, Sobol's sequence, is adopted in this paper.

It needs to be realized that points ($\widetilde{\boldsymbol{X}_i}$) in low-discrepancy samples are not independent of each other. Therefore, the central limit theorem does not hold for Q_{qmc}, and the confidence interval defined in Eq. (2) cannot be used. Instead, a randomized quasi-Monte Carlo method can be applied. The idea of RQMC is to create m random samples of Q_{qmc}, each based on m randomized low-discrepancy point sets of size n. The randomized low-discrepancy point sets can be obtained from Sobol's sequences by scrambling and permutation [13], and the m Q_{qmc} can be considered m i.i.d. samples drawn from the population distribution of Q_{qmc}. As a result, an RQMC estimator Q_{rqmc} can be defined as the mean of the m quasi-random estimators (i.e., $Q_{rqmc} = \frac{1}{m}\sum_{l=1}^{m} Q_{qmc,l}$), and the central limit theory can be applied to Q_{rqmc}. The variance of Q_{rqmc} can be estimated with $\hat{\sigma}^2_{m,rqmc} = \frac{1}{m}\hat{\sigma}^2_{rqmc}$, where $\hat{\sigma}^2_{rqmc} = \frac{1}{m-1}\sum_{l=1}^{m}\left(Q_{qmc,l} - Q_{rqmc}\right)^2$. The total number of model evaluations in RQMC is mn, and m and n are taken as 10 and 512,

respectively, in this paper. In theory, n should be taken as large as possible to reduce the variance of the quasi-random estimators, and m needs to be sufficiently large ($m \geq 10$) to achieve a reliable estimation of $\hat{\sigma}^2_{m,rqmc}$ [23].

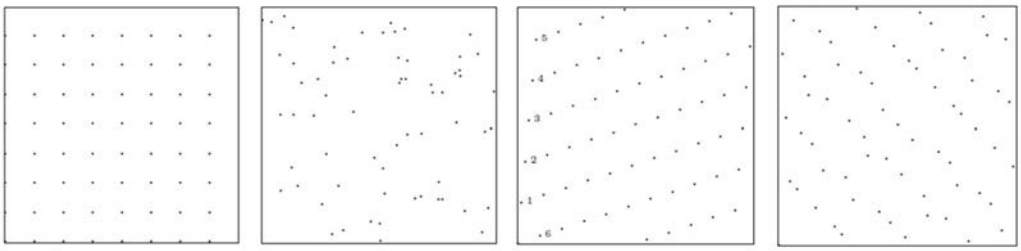

(a) (b) (c) (d)

Figure 2: Four different DOE point sets with 64 samples (a) trapezoidal rule; (b) crude MC; (c) A low-discrepancy point set constructed with Korobov lattices; (d) A low-discrepancy point set constructed with Sobol's sequence (after [22]).

3.4 Performance of the MFMC and RQMC methods

Fig. 3 compares the evolution of $p_{f,A}$ and $p_{f,B}$ with the number of model evaluations between the crude MC and MFMC methods. It can be observed that $p_{f,A}$ and $p_{f,B}$ estimated with the MFMC method are very close to the values estimated with the crude MC method, but the 95% confidence interval (CI) half-width bandwidths of the MFMC estimators are much smaller than the crude MC estimators. The values of $p_{f,A}$ and $p_{f,B}$ estimated with the MFMC method at a small sample size are also closer to the final estimations than the crude MC method. This implies that the MFMC method needs fewer model evaluations to achieve the same level of accuracy as the crude MC method. The computation times and efficiencies are reported in Table 2 and Table 3. ε_A and ε_B are two outputs from the structural analysis model, so the computation time for each method is the same in Table 2 and Table 3. The computation time in the MFMC method is longer than the crude MC method because of the additional evaluations of the lower-fidelity model. Building A in the SAM shows weak nonlinearity, and the correlation coefficient between the linear and nonlinear models is around 0.7. In contrast, building B shows stronger nonlinearity, and the correlation coefficient between linear and nonlinear models is around 0.5. Since a strong correlation between multi-fidelity models is preferred in the MFMC method, the efficiency of building A increased more from the MFMC method.

Fig. 4 compares the convergence of the crude MC method and the RQMC method. The $p_{f,A}$ and $p_{f,B}$ estimated with RQMC also show smaller confidence intervals than the crude MC method. The computation time and efficiency are also reported in Table 2 and Table 3. The computation time is slightly larger than the crude MC method because around 100 more model evaluations are required in the RQMC method. However, the efficiency for estimating both $p_{f,A}$ and $p_{f,B}$ improved significantly, and the efficiency improvement of $p_{f,A}$ is more significant than $p_{f,B}$. To better study the convergence rate of $p_{f,A}$ and $p_{f,B}$, another 5120 quasi-random samples are generated (i.e., $m = 20$) and evaluated with the SAM for a better estimation of $\hat{\sigma}^2_{rqmc}$. A log2-log2 plot is then produced for the 95% confidence half-width bandwidths of the crude MC and $Q_{qmc,l}$ in Fig. 5. As suggested in [24-25], RQMC can also reduce the estimator variance because:

$$\mathrm{Var}\left[Q_{qmc,l}\right] = \frac{\mathrm{Var}\left[f(\widetilde{\boldsymbol{X}}_l)\right]}{n} + \frac{2}{n^2}\sum_{i<j}\mathrm{Cov}\left[f\left(\widetilde{\boldsymbol{X}}_i\right), f\left(\widetilde{\boldsymbol{X}}_j\right)\right] \tag{6}$$

and $\mathrm{Cov}\left[f(\widetilde{\boldsymbol{X}}_i), f(\widetilde{\boldsymbol{X}}_j)\right]$ is generally pairwise negative in the RQMC method. Fig. 5 shows that the variance reduction effect for estimating $p_{f,A}$ is more significant than $p_{f,B}$. This may again because the nonlinearity in building A is weaker than building B, and $\widetilde{\boldsymbol{X}}_i$ and $\widetilde{\boldsymbol{X}}_j$ are better separated after transformed by f (i.e., the SAM). $p_{f,B}$ shows a larger convergence rate than $p_{f,A}$, and this may be because the SAM of building B is "smoother" than building A. Quasi-MC methods can usually achieve faster convergence when the integrand is "smoother." However, the "smoothness" is defined based on the derivative of $f(\boldsymbol{X})$ and is hard to be examined for the SAM in this paper.

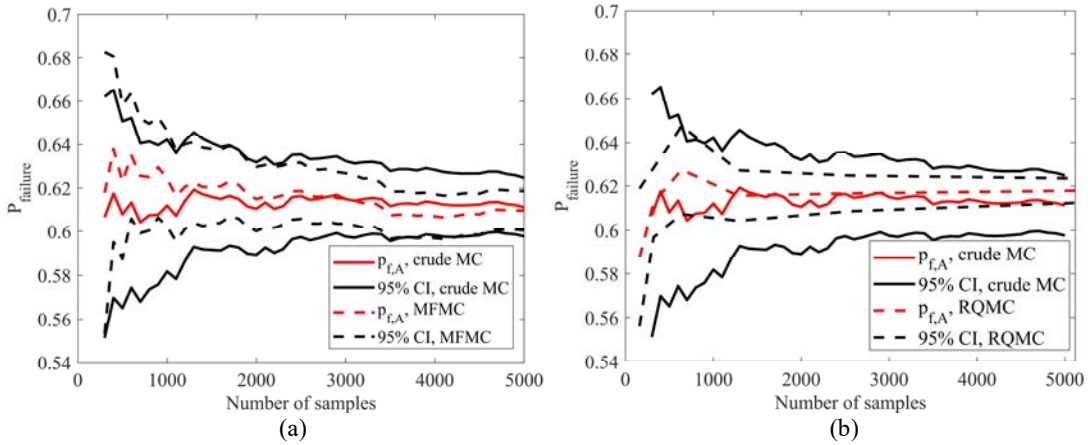

Figure 3: Convergence of crude MC and MFMC (a) evolution of $p_{f,A}$; (b) evolution of $p_{f,B}$.

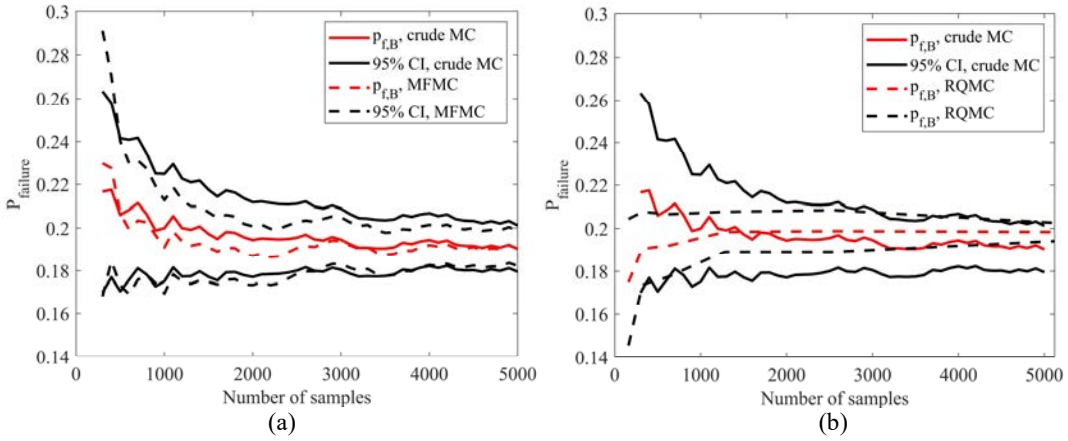

Figure 4: Convergence of crude MC and RQMC (a) evolution of $p_{f,A}$; (b) evolution of $p_{f,B}$.

Method	$p_{f,A}$	HW	Time (min)	Efficiency	Efficiency improvement
Crude MC	61.12%	1.35%	126.6	166.19	0%
MFMC	60.97%	0.9%	169.8	281.13	69.16%
RQMC	61.86%	0.79%	151.2	408.26	145.66%

Table 2: Comparison of MC estimators for $p_{f,A}$, where HW is the half-width of a 95% confidence interval.

Method	$p_{f,B}$	HW	Time (min)	Efficiency	Efficiency improvement
Crude MC	19.04%	1.09%	126.6	256.19	0%
MFMC	19.06%	0.83%	169.8	329.40	28.58%
RQMC	19.84%	0.64%	151.2	438.68	71.23%

Table 3: Comparison of MC estimators for $p_{f,B}$, where HW is the half-width of a 95% confidence interval.

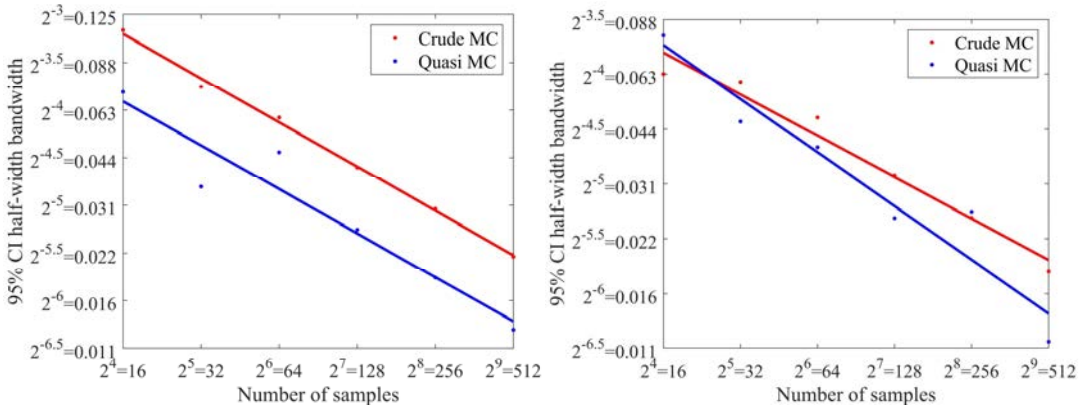

Figure 5: Convergence rate of crude MC and QMC, left: $p_{f,A}$; right: $p_{f,B}$

4 CONCLUSIONS

This paper presents a benchmark problem of high-dimensional uncertainty propagation in deep excavation engineering involving random field models and nonlinear structural analysis models. Numerical experiments are conducted to compare the crude MC method, multi-fidelity MC method, and randomized quasi-MC method in the benchmark problem. It was found that the MFMC method improved the numerical integration efficiency by 30-70%, and the RQMC method improved the efficiency by 70-140%. The performance of the MFMC method depends on the correlation between the lower- and higher-fidelity models. A more considerable efficiency improvement can be achieved if a lower-fidelity model strongly correlated to the higher-fidelity model can be constructed. On the other hand, the performance of the RQMC method may depend on the integrand (the structural analysis model) in the numerical integration. A "smoother" SAM with weaker nonlinearity may benefit more from the RQMC method. In practice, a lower-fidelity model needs to be developed for the MFMC method, while the RQMC method is easier to implement. Quasi-random number generators can be found in many scientific computing platforms, such as Python, R, Matlab, and C++. Simply replacing pseudo-random generators with quasi-random generators may significantly increase the efficiency of uncertainty propagation. However, the number of samples in RQMC needs to be carefully selected (e.g., Sobol's sequence requires the sample size to be a power of 2), and the estimation of variance is not as trial as the crude MC method. Nevertheless, both MFMC and RQMC methods show promising potential in geotechnical engineering and broader civil infrastructure engineering applications.

5 REFERENCES

[1] Pan, Y., Yao, K., Phoon, K. K., & Lee, F. H. (2019). Analysis of tunnelling through spatially-variable improved surrounding–A simplified approach. *Tunnelling and Underground Space Technology*, *93*, 103102.

[2] Goh, A. T., Zhang, W. G., & Wong, K. S. (2019). Deterministic and reliability analysis of basal heave stability for excavation in spatial variable soils. *Computers and Geotechnics*, *108*, 152-160.

[3] Cheng, H., Chen, J., & Li, J. (2019). Probabilistic analysis of ground movements caused by tunneling in a spatially variable soil. *International Journal of Geomechanics*, *19*(12), 04019125.

[4] Zhang, W., Han, L., Gu, X., Wang, L., Chen, F., & Liu, H. (2022). Tunneling and deep excavations in spatially variable soil and rock masses: A short review. *Underground Space*, 7(3), 380-407.

[5] Zhao, J., Ritter, S., DeJong, M.J., (2023). Framework to enable regional 3D probabilistic assessment of excavation induced structural damage using a Monte-Carlo Method, *Proceeding to Geo-risk 2023.*

[6] Zhao, J., & DeJong, M. (2023). Three-dimensional probabilistic assessment of tunneling induced structural damage using Monte-Carlo method and hybrid finite element model. *Computers and Geotechnics*, *154*, 105122.

[7] Zhao, J., Ritter, S., & DeJong, M. J. (2022). Early-stage assessment of structural damage caused by braced excavations: Uncertainty quantification and a probabilistic analysis approach. *Tunnelling and Underground Space Technology*, *125*, 104499.

[8] Schuster, M., Kung, G. T. C., Juang, C. H., & Hashash, Y. M. (2009). Simplified model for evaluating damage potential of buildings adjacent to a braced excavation. *Journal of geotechnical and geoenvironmental engineering*, *135*(12), 1823-1835.

[9] Cami, B., Javankhoshdel, S., Phoon, K. K., & Ching, J. (2020). Scale of fluctuation for spatially varying soils: estimation methods and values. *ASCE-ASME Journal of Risk and Uncertainty in Engineering Systems, Part A: Civil Engineering*, 6(4), 03120002.

[10] Moustapha, M., Fajraoui, N., Marelli, S., & Sudret, B., UQLab user manual – Random fields, Report UQLab-V2.0-119, Chair of Risk, Safety and Uncertainty Quantification, ETH Zurich, Switzerland, 2022.

[11] Son, M., & Cording, E. J. (2007). Evaluation of building stiffness for building response analysis to excavation-induced ground movements. *Journal of geotechnical and geoenvironmental engineering*, *133*(8), 995-1002.

[12] Lemieux, C. (2008). Pseudorandom Number Generators. In *Monte Carlo and Quasi-Monte Carlo Sampling* (pp. 57-85). New York, NY: Springer New York.

[13] Owen, A. B. (1997). Scrambled net variance for integrals of smooth functions. *The Annals of Statistics*, *25*(4), 1541-1562.

[14] Joe, S., & Kuo, F. Y. (2008). Constructing Sobol sequences with better two-dimensional projections. *SIAM Journal on Scientific Computing*, *30*(5), 2635-2654.

[15] Joe, S & Kuo, F.Y. (2010). *Sobol sequence generator*. University of New South Wales. Retrieved 02-13-2023, from https://web.maths.unsw.edu.au/~fkuo/sobol/.

[16] Lemieux, C. (2008). Variance Reduction Techniques. In *Monte Carlo and Quasi-Monte Carlo Sampling* (pp. 87-136). New York, NY: Springer New York.

[17] Peherstorfer, B., Willcox, K., & Gunzburger, M. (2018). Survey of multifidelity methods in uncertainty propagation, inference, and optimization. *Siam Review*, *60*(3), 550-591.

[18] Peherstorfer, B., Beran, P. S., & Willcox, K. E. (2018). Multifidelity Monte Carlo estimation for large-scale uncertainty propagation. In 2018 AIAA Non-Deterministic Approaches Conference (p. 1660).

[19] Patsialis, D., & Taflanidis, A. A. (2021). Multi-fidelity Monte Carlo for seismic risk assessment applications. *Structural Safety*, *93*, 102129.

[20] Niederreiter, H. (1992). *Random number generation and quasi-Monte Carlo methods*. Society for Industrial and Applied Mathematics.

[21] Bellman, R. (1961). *Adaptice Control Processes: A Guided Tour.* Princeton University Press, Princeton, NJ.

[22] Lemieux, C. (2008). Quasi-Monte Carlo Constructions. In *Monte Carlo and Quasi-Monte Carlo Sampling* (pp. 139-197). New York, NY: Springer New York.

[23] Lemieux, C. (2008). Using Quasi-Monte Carlo in Practice. In *Monte Carlo and Quasi-Monte Carlo Sampling* (pp. 201-249). New York, NY: Springer New York.

[24] L'Ecuyer, P., & Lemieux, C. (2002). Recent advances in randomized quasi-Monte Carlo methods. *Modeling uncertainty: An examination of stochastic theory, methods, and applications*, 419-474.

[25] L'Ecuyer, P. (2018). *Randomized quasi-Monte Carlo: An introduction for practitioners* (pp. 29-52). Springer International Publishing.